# Design of an Active Fragment of a Class II Aminoacyl-tRNA Synthetase and Its Significance for Synthetase Evolution†

John Augustine and Christopher Francklyn*

*Department of Biochemistry, University of Vermont College of Medicine, Health Sciences Complex, Burlington, Vermont 05405*

*Received September 23, 1996; Revised Manuscript Received December 23, 1996*⊗

ABSTRACT: Primordial aminoacyl-tRNA synthetases (aaRSs) based on the Rossman nucleotide binding fold of class I enzymes or the seven-stranded antiparallel $\beta$-sheet fold of class II enzymes have been proposed to predate the contemporary aaRS. As part of an inquiry into class II aaRS evolution, the individual domains of the homodimeric *Escherichia coli* histidyl-tRNA synthetase (HisRS) were separately expressed and purified to determine their individual contributions to catalysis. A 320-residue fragment ($N_{cat}$ HisRS) truncated immediately following motif 3 catalyzes both the specific aminoacylation of tRNA and pyrophosphate exchange, albeit less efficiently than the full-length enzyme. $N_{cat}$ HisRS showed no mischarging of noncognate tRNAs but exhibited reduced selectivity for the C73 discriminator base, a principal aminoacylation determinant for histidine tRNAs. Size exclusion chromatography showed that $N_{cat}$ HisRS is monomeric, indicating that the C-terminal domain is essential for maintaining the dimeric structure of the enzyme. The stably folded C-terminal domain ($C_{ter}$ HisRS) was inactive for both reactions and did not enhance the activity of $N_{cat}$ HisRS when added *in trans*. The fusion of one or more accessory domains to a primordial catalytic domain may therefore have been a critical evolutionary step by which aminoacyl-tRNA synthetases acquired increased catalytic efficiency and substrate specificity.

Owing to their essential role in the translation of genetic information, the aminoacyl-tRNA synthetases (aaRSs)[1] are likely to have arisen early in evolution (Carter, 1993; Nagel & Doolittle, 1991; Schimmel et al., 1993). These enzymes catalyze a two-step reaction in which the cognate amino acid is activated by condensation with ATP and subsequently transferred to the terminal adenosine of the cognate tRNA (Schimmel & Söll, 1979). In order to carry out these reactions with the fidelity required for protein synthesis *in vivo*, the aaRSs have acquired diverse structural features to select their cognate tRNA and amino acid substrates from a pool of similar molecules (Arnez & Moras, 1995; Cusack, 1995; Delarue, 1995). At least part of the selection process is associated with elaborate proofreading mechanisms (Fersht, 1977; Schmidt & Schimmel, 1995). By contrast, the recognition of the universal substrate ATP is mediated through signature sequences which comprise essential components of one of two different catalytic folds, providing a basis for division of the aaRS into two distinct classes with a number of subgroups. The class I enzymes share a common "Rossman nucleotide-binding fold" characterized by five parallel $\beta$-strands and four $\alpha$-helices (Carter, 1993), while the class II enzymes possess a seven-stranded antiparallel $\beta$-sheet buttressed by three $\alpha$-helices (Cusack et al., 1990). In addition to providing the structural basis for ATP recognition, the two classes also differ in the regiochemistry of the ultimate attachment of the amino acid to the tRNA 3′ terminus.

With the conservation of the class specific catalytic domains firmly established in some eleven representative crystal structures, increasing attention is now being focused on the specialized protein domains that augment the catalytic cores (Delarue & Moras, 1993). These include both variable-length insertions that split the core domain and accessory domains appended to the N and C termini of the cores. The insertion and accessory domains are generally specific only to the evolutionary family of aaRSs that recognize the same amino acid substrate (Cusack et al., 1991; Landes et al., 1995), but topological conservation of accessory domains among the aaRSs in the same subgroup has recently been noted for both class IIa and class IIb enzymes (Arnez et al., 1995; Logan et al., 1995; Onesti et al., 1995).

A major function of the accessory domain(s) suggested from the cocrystal structures reported is sequence specific interaction with cognate tRNAs. The coiled-coil domains of SerRS provide sequence specific recognition of the long variable arm of the isoaccepting seryl-tRNAs (Biou et al., 1994), while the $\beta$-barrel domains of AspRS and GlnRS serve as anticodon binding motifs (Cavarelli et al., 1993; Rould et al., 1991). The acceptor binding domain inserted into the Rossman fold of GlnRS provides further tRNA specificity through the stabilization of an unusual conformation of the tRNA acceptor stem consisting of an unpaired U1·A72 base pair and a bent CCA terminus (Rould et al., 1989). These structural and functional relationships among the aaRSs which belong to the same class have prompted a number of investigators to propose that aaRS originated from primordial enzymes consisting of either the class I or class

† This investigation was supported by USPHS NIH Grant GM 48146.

* To whom correspondence should be addressed: Professor Christopher Francklyn, Department of Biochemistry, University of Vermont College of Medicine, Health Sciences Complex C444, Burlington, VT, 05405. Telephone: (802)-656-8450; Fax: (802)-862-8229.

⊗ Abstract published in *Advance ACS Abstracts,* March 15, 1997.

[1] Abbreviations: aaRS, aminoacyl-tRNA synthetase; HPLC, high-pressure liquid chromatography; IPTG, isopropyl 1-thio-$\beta$-D-galactopyranoside; HEPES, *N*-(2-hydroxyethyl)piperazine-*N*′-2-ethanesulfonic acid; Ni-NTA, nickel nitrilotriacetic acid; NOESY, nuclear Overhauser enhancement spectroscopy; PCR, polymerase chain reaction. Following the standard convention, aminoacyl-tRNA synthetases are referred to by the three-letter code for their amino acid substrate, followed by the suffix RS.

S0006-2960(96)02395-1 CCC: $14.00 

II catalytic fold, which subsequently acquired the distinctive accessory domains of modern aaRS (Rould et al., 1989; Schimmel et al., 1993; Cusack, 1993).

With these considerations in mind, we chose to examine the individual catalytic contributions of the N-terminal catalytic and C-terminal accessory domains of a class II aaRS using histidyl-tRNA synthetase from *Escherichia coli* as a model system (Arnez et al., 1995). The crystal structure of this 96 kDa homodimer reveals that HisRS has a relatively simple modular organization in which the N-terminal class II catalytic domain is joined via a short flexible linker to a C-terminal domain composed of a mixed parallel/antiparallel $\beta$-structure. This accessory domain interacts exclusively with the core domain of the other monomer, providing another potentially significant dimeric interface in addition to the canonical motif 1 interface. A recent genetic and biochemical analysis showed that the C-terminal domain and its interface with the catalytic domain are important for selection of cognate tRNA *in vivo* (Yan et al., 1996). In the studies described here, we investigated the enzymatic capabilities of the isolated N-terminal catalytic (1−320 $N_{cat}$ HisRS) and C-terminal (330−424 $C_{ter}$ HisRS) domains and their potential for noncovalent association. Through the determination of steady state kinetic parameters of the pyrophosphate exchange and aminoacylation reactions, the energetic contributions of each domain to catalysis were estimated. This analysis provides insights into possible models for synthetase evolution.

## MATERIALS AND METHODS

*Materials*. Restriction enzymes and other molecular biology reagents were obtained from New England Biolabs or Boehringer and were used according to the manufacturer's protocols. The Ni-NTA affinity resin was purchased from Qiagen.

*Bacterial Strains and Plasmids.* To express the independent domains of HisRS, DNA fragments encoding amino acids (aa) 1−320 and amino acids 330−424 were amplified by PCR using primers encoding unique *Bam*HI-*Hin*dIII and *Nco*I-*Bgl*II restriction sites at the ends of the *hisS* (aa 1−320) and *hisS* (aa 330−424) DNA fragments, respectively. Following digestion with the appropriate enzymes, the *hisS* (aa 1−320) PCR product was introduced into the *Bam*HI-*Hin*dIII sites of plasmid pQE-30 (Qiagen), which contains a multiple cloning site downstream of a leader sequence encoding six tandem histidine residues to permit purification by affinity chromatography. The DNA fragment encoding the COOH-terminal domain (aa 330−424) of HisRS was cloned into the *Nco*I-*Bgl*II sites of plasmid pQE-60 (Qiagen), which contains a multiple cloning site upstream of the leader sequence encoding six tandem histidine residues. Previously, it has been shown that the presence of the affinity tag does not significantly affect the aminoacylation activity of HisRS (Yan et al., 1996). The pQE-60 vector was chosen in order to place the $His_6$ affinity tag at the C terminus of this domain, and thus avoid the introduction of polar residues into a region where packing interactions with the N-terminal domain might be disrupted. Both constructs were confirmed by DNA sequencing. The full-length affinity-tagged HisRS construct has been described previously (Yan et al., 1996). Bacterial strain JM105 was used as the background for the expression of all HisRS proteins.

*Protein Expression and Purification.* T7 RNA polymerase was purified from strain pAR1219/BL-21 by the method of Grodberg and Dunn (1988). The full-length, $N_{cat}$, and $C_{ter}$ HisRS proteins were overexpressed and purified by the use of the QIAExpress System (Qiagen) which utilizes Ni-NTA agarose chromatography and requires that the protein of interest possess a $His_6$ fusion tag. *E. coli* JM105 cells carrying the appropriate HisRS plasmids were grown in rich media to log phase at 37 °C before induction by 1 mM IPTG for 4 h. Crude extracts were prepared as described previously (Yan et al., 1996). Briefly, cell extracts were incubated with Ni-NTA resin for 1 h on ice, and then the mixture was transferred to a 10 mL column. Proteins that were bound nonspecifically were eliminated with wash buffer [50 mM potassium phosphate (pH 6.0), 300 mM NaCl, 10 mM $\beta$-mercaptoethanol, and 10% glycerol] until the $A_{280}$ of the eluate was below 0.1. Affinity-tagged proteins were then eluted with a gradient of 0 to 0.4 M imidazole in wash buffer. Peak fractions identified by SDS−PAGE were pooled and dialyzed against a buffer containing 50 mM potassium phosphate (pH 7.0), 100 mM KCl, 10% glycerol, and 10 mM $\beta$-mercaptoethanol at 4 °C. Protein was then concentrated to 5 mg/mL in dialysis buffer containing 40% glycerol and then stored at −20 °C. Protein concentrations were initially estimated from the theoretical value of the molar extinction coefficient of each domain (Gill & von Hippel, 1989). The functional concentration of $N_{cat}$ HisRS was determined by active site titration (Fersht et al., 1975), assuming that 1 mol of ATP was hydrolyzed per mole of active sites.

*Western Blotting*. Western blot analysis of sonicated cell lysates of the HisRS constructs was carried out as described previously (Yan et al., 1996) Briefly, equivalent amounts of protein from uninduced cell lysates were separated on a 12.5% SDS−PAGE gel and transferred to Schleicher & Schuell Nytran membranes. Mouse-derived $^{MRGS}$·His antibody (Qiagen) was used for detecting recombinant proteins containing the epitope $MRGS(His)_6$. Goat anti-mouse IgG conjugated with horseradish peroxidase secondary antibody (Pierce) was incubated with the immobilized $^{MRGS}$·His antibody. Subsequent addition of Renaissance Western Blot Chemiluminescence Reagent (DuPont) allowed for protein visualization by autoradiography.

*NMR Spectroscopy*. The $C_{ter}$ HisRS sample for NMR spectroscopy was prepared in an aqueous solution at a protein concentration of 1 mM in a buffer containing 20 mM $KH_2PO_4$ (pH 7.0) and 300 mM KCl. NMR spectra were obtained with a Varian Unity Plus 500 spectrometer using a sample temperature of 20 °C. The NOESY spectrum was acquired using pulse sequences described elsewhere (Jeener et al., 1979). The total experimental time was 16 h.

*$PP_i$ Exchange Assay*. Inorganic pyrophosphate exchange reactions were performed according to Calender and Berg (1966). Assay reaction mixtures contained 100 mM Tris (pH 8.0), 10 mM $\beta$-mercaptoethanol, 10 mM KF, 10 mM $MgCl_2$, 2 mM [$^{32}$P]$NaPP_i$, 500 nM $N_{cat}$ HisRS, 10−500 $\mu$M histidine, and 10−2000 $\mu$M ATP. Saturating concentrations of ATP and histidine were 2 mM. Reaction mixtures of 1 mL were incubated at 37 °C for up to 20 min and quenched with 4 volumes of 7% perchloric acid containing 10 mM $NaPP_i$. Activated charcoal was added, and [$^{32}$P]ATP was separated by filtration through glass filter pads (Whatman).

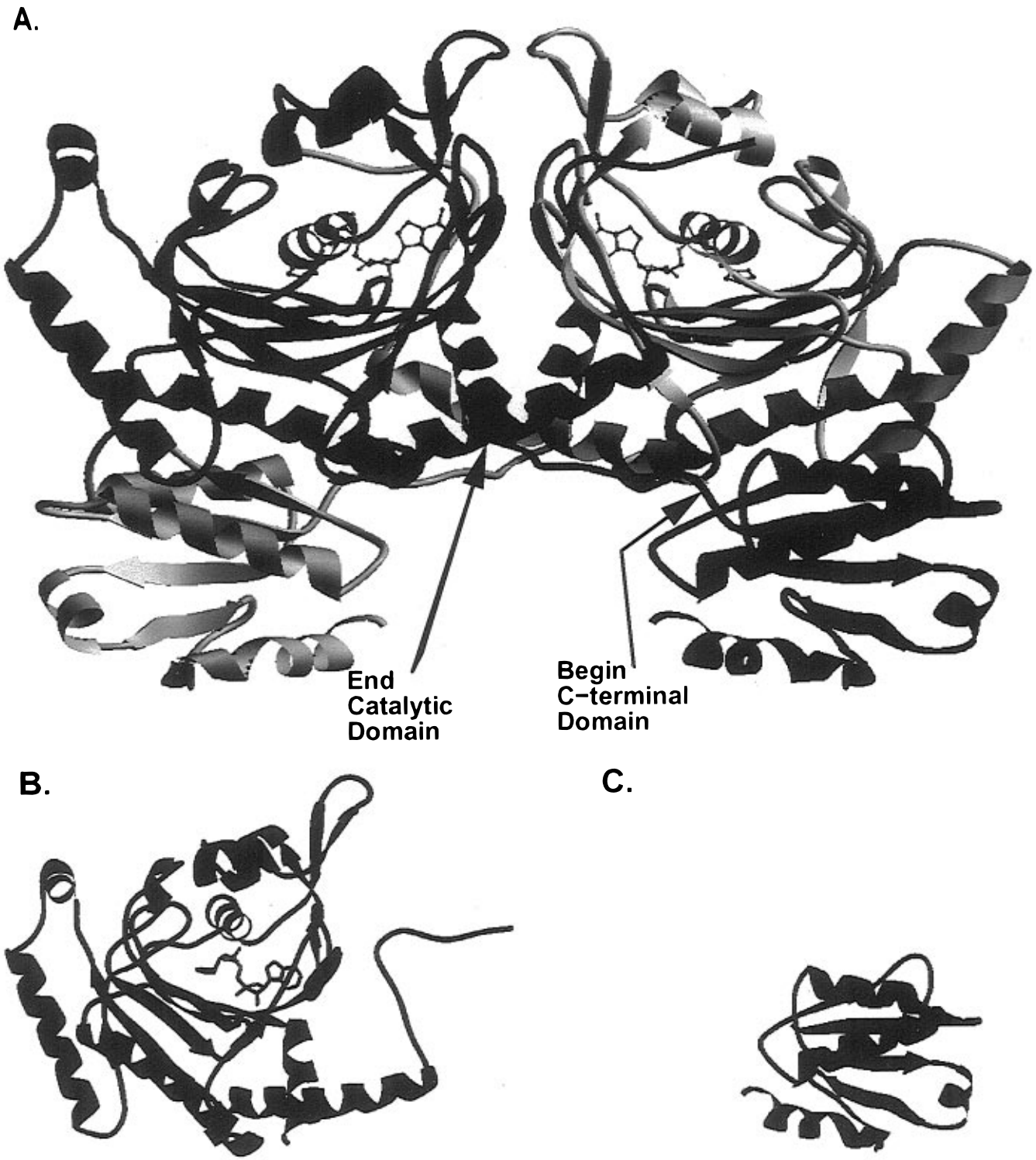


FIGURE 1: Ribbon diagram of the X-ray structure from the adenylate complex of *E. coli* HisRS (Arnez et al., 1995). The arrows in panel A indicate the end of the coding sequence for $N_{cat}$ HisRS (B) and the beginning of $C_{ter}$ HisRS (C).

*Synthesis of tRNA$^{His}$ in Vitro Transcripts*. The construction of the plasmid templates for T7 RNA polymerase *in vitro* synthesis of wild-type tRNA$^{His}$ and the C73 tRNA$^{His}$ amber suppressor has been described previously (Yan et al., 1996). The construction of the eight-base pair microhelix template, which recapitulates the acceptor helix of tRNA$^{His}$, has also been described previously (Francklyn & Schimmel, 1990). Plasmid DNAs were purified by $CsCl_2$ gradients prior to *in vitro* tRNA synthesis. The tRNA transcripts were prepared according to standard published protocols (Yan et al., 1996). The concentration of each tRNA transcript preparation was determined by its specific histidine acceptance, typically 1200 pmol/$A_{260}$.

*In Vitro Aminoacylation Assays*. Aminoacylation of tRNA$^{His}$ transcripts by the pure full-length and $N_{cat}$ HisRS proteins was carried out as described previously (Yan et al., 1996; Francklyn et al., 1992). Standard aminoacylation reactions were performed in a buffer containing 50 mM HEPES (pH 7.5), 100 mM KCl, 8.3 mM DTT, 2.5 mM ATP, 10 mM $MgCl_2$, 22.4 $\mu$M [$^3$H]histidine, and varying amounts of enzyme and tRNA. The reaction mixtures were incubated at 37 °C and terminated by quenching with trichloroacetic

acid-soaked 3MM filters (Whatman). The specific activity of the tritiated amino acid was corrected for the variation in scintillation counting efficiency for the free amino acid versus the amino acid esterified to the tRNA (Francklyn et al., 1992).

*Size Exclusion Chromatography*. Gel filtration HPLC of purified HisRS protein preparations was performed on a Waters 501 series HPLC system equipped with a ToSoHaas TSK-G2000 SWXL size exclusion column. Before sample application, the column was equilibrated in 100 mM potassium phosphate (pH 7.2), 300 mM KCl, and 1 mM DTT at a flow rate of 1 mL/min. The column void volume was determined from the elution volume of blue dextran (Pharmacia). One hundred microliters of 2 mg/mL solutions of various low-molecular mass standards (Pharmacia) was injected onto the column, and the optical density of eluted proteins was detected by a Waters 481 UV photometer connected in series with the HPLC system. Using the formula $K_{av} = (V_e - V_o)/(V_t - V_o)$, where $V_e$, $V_o$, and $V_t$ represent the elution, void, and column volumes, respectively, the $K_{av}$ of each protein standard was determined and plotted versus the log of its molecular mass. Exclusion chromatography experiments were then performed on purified HisRS proteins, and their molecular masses were determined from the value of $K_{av}$ using the standard curve.

## RESULTS

*Expression and Purification of Isolated HisRS Domains*. On the basis of the structure of the HisRS−adenylate cocrystal complex from *E. coli* (Arnez et al., 1995), each monomeric subunit of HisRS consists of an N-terminal catalytic domain connected to an independent C-terminal domain by a short peptide linker (Figure 1). This linker immediately follows motif 3 (300−320), such that the N-terminal domain possesses all three of the canonical class II motifs. Cleavage of the protein at the peptide linker would be predicted to bisect the protein into its component domains. Limited proteolysis of HisRS by a variety of proteases leads to preferential cleavage at Glu 55, suggesting that the amino acid 320−330 linker region is not easily accessible to proteases (C. Francklyn, unpublished results). Therefore, standard molecular biology techniques were used to produce the two domains independently. The DNA fragments corresponding to the N-terminal 1−320 amino acids and the C-terminal 330−424 amino acids were cloned into the *Bam*HI-*Hin*dIII and *Nco*I-*Bgl*II sites of the $His_6$ affinity tag vectors pQE-30 and pQE-60, respectively. These plasmids were then used to separately transform *E. coli* JM105 cells. When induced by the addition of 1 mM IPTG, both proteins accumulated to high levels as determined from analysis of crude extracts on SDS−PAGE. This overproduction permitted purification with only slight modification of procedures used for the full-length protein, as described in Materials and Methods. The purified proteins migrated on SDS−PAGE gels at the expected sizes of 35 kDa for the N-terminal domain ($N_{cat}$ HisRS) and 11 kDa for the C-terminal domain ($C_{ter}$ HisRS) (Figure 2). The successful expression and purification of each domain separately suggests that each represents an independently folded polypeptide with considerable global stability. Further evidence for the stability of the N-terminal domain was provided by Western blot analysis, which revealed that $N_{cat}$ HisRS accumulated to *in vivo* levels approaching that of the full-length protein under uninduced conditions (Figure 2).

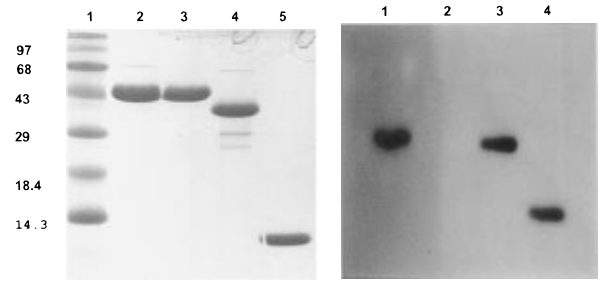


FIGURE 2: Expression of isolated $N_{cat}$ HisRS and $C_{ter}$ HisRS domains. Purification of the two domains of HisRS was carried out as in Materials and Methods. Purified protein was separated by SDS−PAGE and visualized by Coomassie staining (left panel): lane 1, protein standards; lanes 2 and 3, untagged and $His_6$-tagged full-length HisRS proteins, respectively, and lanes 4 and 5, purified $N_{cat}$ HisRS and $C_{ter}$ HisRS, respectively. Western blot analysis (right panel) from various uninduced pQE-30 cell extracts was carried out as described in Materials and Methods: lane 1, 5 $\mu$g of purified $His_6$-tagged full-length HisRS; lane 2, 15 $\mu$g of uninduced cell extract from $His_6$ vector pQE-30; lane 3, 15 $\mu$g of uninduced cell extract from full-length HisRS/pQE-30. Lane 4, 15 $\mu$g of uninduced cell extract from $N_{cat}$ HisRS/pQE-30.

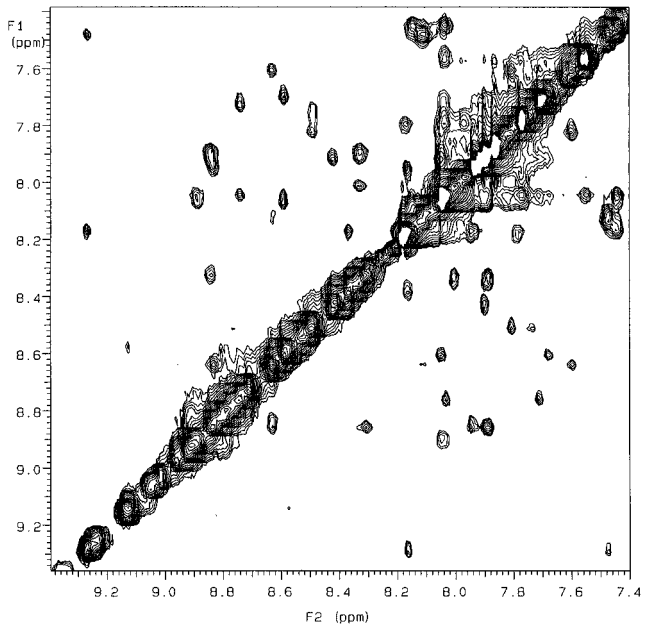


FIGURE 3: Two-dimensional 200 ms mixing time NOESY spectrum of the amide region of $C_{ter}$ HisRS. Experimental conditions were as described in Materials and Methods.

*$C_{ter}$ HisRS Is a Stably Folded Domain*. The absence of the MRGS$(His)_6$ epitope tag in the $C_{ter}$ HisRS construct precluded detection of this domain by Western blot analysis. Therefore, in order to determine if $C_{ter}$ HisRS was stably folded, one-dimensional (1D) NMR and two dimensional (2D) NOESY NMR experiments were performed. The large chemical shift dispersion evident in the 1D spectra provided strong evidence for stable folding of the isolated C-terminal domain (data not shown). This was confirmed in 2D NOESY experiments, which indicated a single, stable conformation shown by an abundance of cross-peaks in the amide region of the spectra characteristic of the $i$ to $i + 3$ connectivity patterns of an α-helical protein (Figure 3). These results are consistent with the HisRS crystal structure, where the C-terminal domain fold has three α-helices packed against a four-stranded mixed $\beta$-sheet. This stable folding

Table 1: Apparent Steady State Kinetic Parameters for Pyrophosphate Exchange by Wild-Type and $N_{cat}$ Histidyl-tRNA Synthetases[a]

| | histidine | | | ATP | | |
|---|---|---|---|---|---|---|
| | $K_m$ ($\mu$M) | $k_{cat}$ ($s^{-1}$) | $k_{cat}/K_m$ ($10^6$ $M^{-1}$ $s^{-1}$) | $K_m$ ($\mu$M) | $k_{cat}$ ($s^{-1}$) | $k_{cat}/K_m$ ($10^6$ $M^{-1}$ $s^{-1}$) |
| wt HisRS | $30 \pm 5$ | $142 \pm 5$ | 4.7 | $890 \pm 64$ | $120 \pm 4$ | 0.13 |
| $(His_6)$-HisRS | $14 \pm 1$ | $140 \pm 2$ | 9.9 | $600 \pm 18$ | $110 \pm 13$ | 0.18 |
| $N_{cat}$ HisRS | $46 \pm 14$ | $0.19 \pm 0.01$ | 0.0041 | $740 \pm 44$ | $0.17 \pm 0.01$ | 0.00023 |

[a] $PP_i$ exchange reactions were carried out at 37 °C as described in Materials and Methods. Enzyme concentrations determined from active site titrations were 10 nM wild-type HisRS for both the $His_6$-tagged and untagged proteins and 500 nM for $N_{cat}$ HisRS. The slope of the line for each initial rate at a given substrate was determined by linear regression. The apparent kinetic parameters and standard errors were determined from at least two data sets using the program Enzfitter (Elsevier) utilizing curve fits to the Michaelis−Menten equation.

is also in agreement with the high levels of expression and lack of insoluble inclusion material observed for $C_{ter}$ HisRS.

*ATP−$PP_i$ Exchange.* As a first step toward determining the extent of catalytic activity retained by the isolated domains of HisRS, pyrophosphate exchange assays were performed. As shown in Table 1, removal of the C-terminal domain of HisRS was accompanied by a 780−2400-fold decrease in the apparent second-order rate constant $k_{cat}/K_m$, suggesting that this domain contributes to the catalysis of the pyrophosphate exchange reaction. This decreased catalytic activity is not likely to be the result of the loss of folding or decreased stability, because the $K_m$ parameters for ATP and histidine were within 1−3-fold of those of the full-length protein (Table 1). The pyrophosphate exchange activity of $N_{cat}$ HisRS was not stimulated by the addition of $C_{ter}$ HisRS, which possessed no intrinsic $PP_i$ exchange activity of its own (data not shown). These results suggests that $C_{ter}$ HisRS is not capable of noncovalent association with $N_{cat}$ HisRS or, if so, this association provides no measurable catalytic benefit.

*In Vitro Aminoacylation Studies.* The $tRNA^{His}$ aminoacylation function of $N_{cat}$ HisRS was examined in a series of assays using catalytic amounts of $N_{cat}$ HisRS and substrate levels of $tRNA^{His}$. These studies showed that $tRNA^{His}$ is aminoacylated with histidine by $N_{cat}$ HisRS, although at a rate decreased relative to that of full-length HisRS (Figure 4A). When $C_{ter}$ HisRS protein was added *in trans* to aminoacylation reaction mixtures containing $N_{cat}$ HisRS, no increase in charging was observed, nor was catalytic activity observed when $C_{ter}$ HisRS was assayed alone (Figure 4B). Thus, $N_{cat}$ HisRS contains all the necessary structural and functional elements necessary to carry out aminoacylation of $tRNA^{His}$. Kinetic parameters for the aminoacylation reaction catalyzed by $N_{cat}$ HisRS were also determined. As shown in Table 2, the relative second-order rate constant $k_{cat}/K_m$ for aminoacylation catalyzed by $N_{cat}$ HisRS was decreased by a factor of 163 relative to that of the full-length HisRS enzyme. This decrease was due entirely to a 406-fold reduction in the $k_{cat}$ parameter. By contrast, the value of $K_m$ for tRNA for $N_{cat}$ HisRS was reduced 2.5-fold relative to that of full-length HisRS. These kinetic parameters were essentially unaltered in the presence of an 8-fold molar excess of $C_{ter}$ HisRS ($k_{cat} = 0.004$ $s^{-1}$; $K_m = 0.19$ $\mu$M), providing further evidence that the C-terminal domain is unable to productively associate with $N_{cat}$ HisRS.

Although these studies on the full-length cognate $tRNA^{His}$ provided strong evidence for the aminoacylation function by $N_{cat}$ HisRS, no conclusions about the retention or loss of tRNA specificity could be drawn. In studies with $tRNA^{Gly}$, neither the full-length nor $N_{cat}$ HisRS proteins showed any mischarging of the noncognate tRNA with histidine (Figure 4A). Likewise, $tRNA^{Ser}$ was not aminoacylated by $N_{cat}$

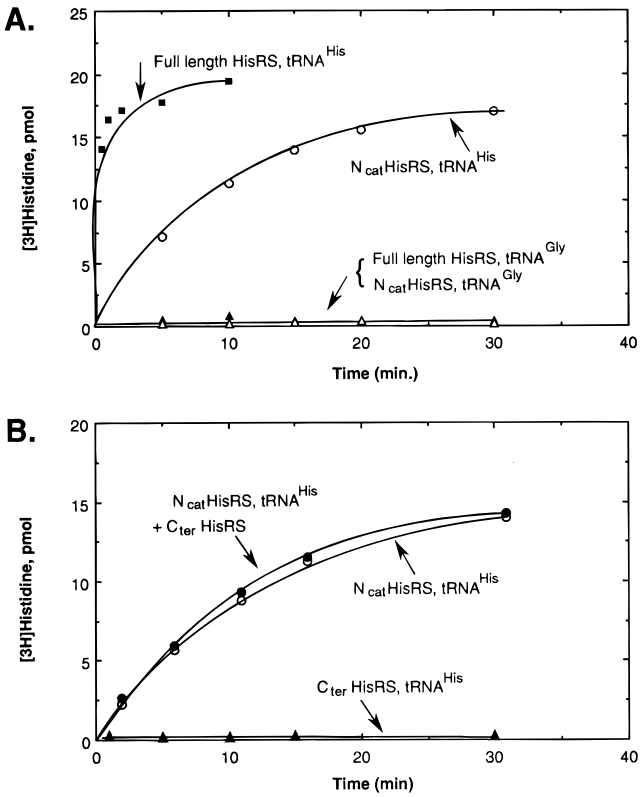


FIGURE 4: Aminoacylation of cognate and noncognate tRNAs with histidine by isolated domains of HisRS at pH 7.5 and 37 °C. The incorporation of [$^3$H]histidine per 10 $\mu$L reaction aliquot is plotted on the ordinate axis: (A) aminoacylation of $tRNA^{His}$ (1 $\mu$M) and $tRNA^{Gly}$ (1 $\mu$M) by full-length HisRS (10 nM) and $N_{cat}$ HisRS (25 nM) and (B) aminoacylation of $tRNA^{His}$ (1 $\mu$M) by $N_{cat}$ HisRS (25 nM) in the presence and absence of $C_{ter}$ HisRS (200 nM).

HisRS (data not shown). To a first approximation, $N_{cat}$ HisRS apparently retains specificity for its cognate tRNA. However, these qualitative assays alone were not sensitive enough to detect more subtle alterations in the recognition of individual determinants. To investigate the tRNA specificity of $N_{cat}$ HisRS more closely, the aminoacylation kinetics for two different $tRNA^{His}$ variants were also determined. The first of these was a variant with the substitution of U for C at position 73, a principal recognition determinant whose substitution decreases the $k_{cat}$ of full-length HisRS by 600-fold (Himeno et al., 1989; Yan & Francklyn, 1994; Yan et al., 1996). The other transcript differed from the wild-type $tRNA^{His}$ by the substitution of the GUG anticodon with CUA, which leads to a 10-fold increase in $K_m$ using full-length HisRS (Yan et al., 1996). In a comparison of $k_{cat}/K_m$ for the U73 discriminator variant, the activity of full-length HisRS was decreased 580-fold, while the corresponding activity for $N_{cat}$ HisRS was decreased only 20-fold (Table 2, compare lines 1 and 3). By contrast, the decrease in

Table 2: Apparent Steady State Kinetic Parameters at 37 °C for Aminoacylation of tRNA by Full-Length and $N_{cat}$ Histidyl-tRNA Synthetases[a]

| | full-length HisRS | | | $N_{cat}$ HisRS | | |
|---|---|---|---|---|---|---|
| RNA substrate | $K_m$ ($\mu$M) | $k_{cat}$ ($s^{-1}$) | $k_{cat}/K_m$ ($10^6$ $M^{-1}$ $s^{-1}$) | $K_m$ ($\mu$M) | $k_{cat}$ ($10^{-2}$ $s^{-1}$) | $k_{cat}/K_m$ ($10^4$ $M^{-1}$ $s^{-1}$) |
| wt $tRNA^{His}$ | $1.4 \pm 0.6$ | $2.6 \pm 0.4$ | 1.8 | $0.56 \pm 0.15$ | $0.64 \pm 0.05$ | 1.1 |
| $tRNA^{His}_{CUA}$ | $13 \pm 0.1$ | $1.5 \pm 0.3$ | 0.11 | $5.5 \pm 3.5$ | $0.26 \pm 0.06$ | 0.048 |
| U73 $tRNA^{His}_{GUG}$ | $1.6 \pm 0.4$ | $0.005 \pm 0.0005$ | 0.0031 | $0.31 \pm 0.04$ | $0.016 \pm 0.0004$ | 0.053 |
| $microhelix^{His}$ | $3.8 \pm 1.9$ | $0.026 \pm 0.004$ | 0.0068 | $4.4 \pm 1.1$ | $0.011 \pm 0.001$ | 0.0026 |

[a] Apparent kinetic parameters for the aminoacylation of wt $tRNA^{His}$ and amber $tRNA^{His}$ (0.1−10 $\mu$M) were determined by measuring the initial rate of charging with 1 nM wt HisRS and 12.5 nM $N_{cat}$ HisRS. Rates for U73 $tRNA^{His}_{GUG}$ (0.2−8.0 $\mu$M) aminoacylation were determined with 100 nM full-length HisRS and 628 nM $N_{cat}$ HisRS. $Microhelix^{His}$ (0.5−25 $\mu$M) initial rates were determined with 50 nM full-length HisRS and 1 $\mu$M $N_{cat}$ HisRS. Initial rate intervals over which data were sampled were determined empirically. Kinetic parameters and standard errors were determined as described in Table 1.

aminoacylation resulting from the introduction of the CUA anticodon was 23-fold for $N_{cat}$ HisRS and 16-fold for the full-length enzyme (Table 2, compare lines 1 and 2). This observation indicates that loss of the C-terminal domain does not eliminate the effect on the $K_m$ parameter that is seen with the full-length HisRS, implying that specificity for the cognate anticodon has not been appreciably diminished in the truncated protein.

HisRS is one of a number of aaRSs that possess the ability to aminoacylate short RNA substrates, such as micro- and minihelices, which are based on the acceptor stem of the cognate tRNA (Martinis & Schimmel, 1995). The efficient aminoacylation of microhelices by HisRS reflects the significant contribution of the acceptor stem to the energetics of aminoacylation (Francklyn et al., 1992). One prediction based on these earlier studies is that loss of the anticodon binding domain should impose less of an effect on the aminoacylation of small helical RNA substrates than on the aminoacylation kinetics of full-length tRNA. To test this hypothesis, the steady state kinetics of aminoacylation were determined with catalytic amounts of $N_{cat}$ HisRS and varying concentrations of $microhelix^{His}$. Parallel reactions with the full-length $His_6$-tagged HisRS were also performed for comparison. The value of $k_{cat}/K_m$ for aminoacylation of $microhelix^{His}$ by $N_{cat}$ HisRS was decreased 423-fold relative to that of the full-length $tRNA^{His}$, as compared to a 265-fold decrease observed with the full-length enzyme (Table 2). The latter value agrees well with the 190-fold decrease in $k_{cat}/K_m$ reported previously (Francklyn et al., 1992). For both enzymes, most of the decrease was attributable to the $k_{cat}$ parameter, but slight differences between full-length and $N_{cat}$ HisRS were observed in the extent of the increase in $K_m$. Thus, both the full-length and truncated HisRS experience similar decreases in activity in the aminoacylation of the microhelix relative to the full-length tRNA, suggesting that both enzymes make one or more productive interactions with sequences outside of the acceptor stem which may contribute to optimal aminoacylation.

*The Catalytic Species of $N_{cat}$ HisRS is Monomeric*. One diagnostic feature of the class II aaRS is motif 1, which is a loose consensus sequence based on a proline-containing g$\phi$xx$\phi$xxP$\phi\phi$ motif. The importance of motif 1 for both the structure of class II aaRS and catalytic function has been demonstrated previously (Eriani et al., 1993). Although HisRS possesses a motif 1 sequence that stabilizes part of the dimeric interface, contacts between the C-terminal domain of one monomer and the N-terminal domain of the other monomer also constitute a substantial dimeric interface (Arnez et al., 1995). Removal of the C-terminal domain

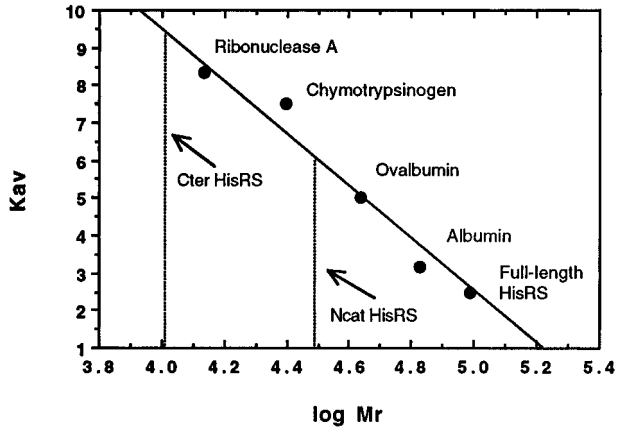


FIGURE 5: Size exclusion chromatography of native $N_{cat}$ HisRS, $C_{ter}$ HisRS, and protein standards (ribonuclease A, 13.7 kDa; chymotrypsinogen, 25 kDa; ovalbumin, 43 kDa; and albumin, 67 kDa). Experimental conditions were as described in Materials and Methods. Log of the molecular mass is plotted versus $K_{av}$. The molecular mass of $N_{cat}$ HisRS and $C_{ter}$ HisRS were determined to be 31.8 and 10.5 kDa, respectively. Full-length HisRS eluted at a molecular mass corresponding to 97 kDa.

might therefore be expected to weaken the dimeric interface. To investigate whether $N_{cat}$ HisRS is monomeric or dimeric, size exclusion experiments using HPLC were conducted both to estimate the solution molecular mass of $N_{cat}$ HisRS and $C_{ter}$ HisRS and to investigate their noncovalent association. The native molecular masses of $N_{cat}$ HisRS and $C_{ter}$ HisRS determined by size exclusion HPLC were 32 and 11 kDa, respectively (Figure 5). These values suggest that both proteins are monomeric in solution. Addition of $C_{ter}$ HisRS to the N-terminal domain gave no change in elution volume of $N_{cat}$ HisRS, providing further evidence for the absence of noncovalent association. The native full-length HisRS protein eluted at a $K_{av}$ corresponding to a molecular mass of 97 kDa (Figure 5), consistent with its dimeric structure. Thus, $N_{cat}$ HisRS is likely to be a monomeric protein under the concentration conditions of the HPLC experiment. On the basis of the amount of $N_{cat}$ HisRS injected (200 $\mu$g) and the column volume (15 mL), a protein concentration of ~430 nM can be estimated for the size exclusion experiment. This was equal to that used in the $PP_i$ exchange assay and at least 20-fold higher than that used in the determination of aminoacylation kinetic parameters. Therefore, $N_{cat}$ HisRS can be assumed to be monomeric under those conditions as well.

Further evidence that the $N_{cat}$ HisRS monomer is the active species was provided by experiments demonstrating a linear relationship between the reaction velocity and enzyme concentration for both the aminoacylation and pyrophosphate

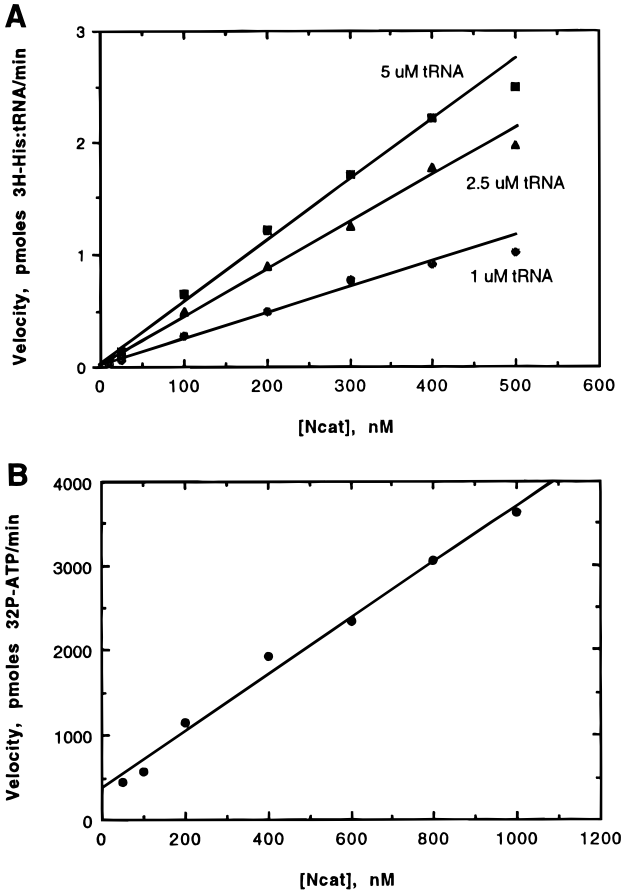


FIGURE 6: Velocity dependence on the $N_{cat}$ HisRS concentration for the aminoacylation and $PP_i$ exchange reactions. (A) Aminoacylation of $tRNA^{His}$ with a 10−500 nM $N_{cat}$ HisRS concentration range was carried out as described in Materials and Methods. (B) $PP_i$ exchange reactions were carried out using a concentration range of 50−1000 $\mu$M $N_{cat}$ HisRS.

exchange reactions (Figure 6). These plots are consistent with the observation that the values of $k_{cat}$ determined for the aminoacylation reaction over a concentration range of 10−500 nM in $N_{cat}$ HisRS were all within 10% of 0.006 $s^{-1}$. If the reduction in $k_{cat}$ observed was purely a reflection of the requirement for the assembly of the two monomers in forming an active dimer, then significant deviations from linearity in the plot of velocity versus enzyme concentration would have been observed, particularly at low enzyme concentrations. This departure from linearity arises from the presence of a quadratic function in the expression relating velocity and total enzyme concentration. The possibility that $N_{cat}$ HisRS undergoes dimerization with a very weak dissociation constant (∼1 mM) is not ruled out, but this association would not be significant under the Michealis−Menten conditions utilized in these kinetic determinations.

*Estimating the Contribution of the C-Terminal Domain to the Apparent Free Energy of Activation for the Pyrophosphate Exchange and Aminoacylation Reactions*. For both the pyrophosphate exchange and aminoacylation reactions, there are distinct transition states that represent the energetic barriers between reactants and products. The apparent differences in the heights of these barriers for the full-length and $N_{cat}$ HisRS can be estimated using the relationship $\Delta\Delta G^{\ddagger} = -RT \ln(k_A/k_B)$, where $\Delta\Delta G^{\ddagger}$ is equal to the difference in the apparent transition state binding energy of the two enzymes and $k_A$ and $k_B$ are operational rate constants which correspond to the $k_{cat}/K_m$ values for the reactions catalyzed by full-length HisRS and $N_{cat}$ HisRS, respectively. Similar treatments have been used to estimate the contribution of individual tRNA domains to the free energy of activation for the aminoacylation reaction (Francklyn et al., 1992; Sampson & Saks, 1993). These analyses require the assumptions that the enzyme obeys Michaelis−Menten kinetics and that the loss of either enzyme or tRNA domains does not affect the energetics of bond-making or -breaking steps. Also, the addition of free energies without a correction term assumes that the contributions of the individual protein or tRNA domains to binding are independent of the contributions of other domains (Fersht, 1985). Although necessarily a simplification, these calculations provide an approximation of the energetic contribution of the various tRNA and aaRS domains to different aaRS−tRNA interactions. In each comparison presented in Table 3, the reaction and the substrate used at various concentrations are identical so that the apparent difference in transition state binding energy between reactions catalyzed by the full-length and truncated enzymes can be calculated. Based on these calculations, the loss of the C-terminal domain was associated with an increase in the activation energy for the aminoacylation reaction on the order of 3.1 kcal $mol^{-1}$. This value represents an estimate of the apparent free energy contribution of the C-terminal domain to transition state stabilization of the aminoacylation of the full-length tRNA. Similar values were obtained for the amber suppressor tRNA and the microhelix for aminoacylation comparisons. By contrast, there was only a difference of 1 kcal $mol^{-1}$ between full-length and $N_{cat}$ HisRS when U73 $tRNA^{His}$ was the substrate, which indicates that the C-terminal domain makes an energetically significant contribution to the discrimination between U73 and C73. Moreover, the C-terminal domain also makes a greater energetic contribution to adenylation than to aminoacylation, as shown by the difference between free energy contributions to the two reactions.

Table 3: Relative Free Energy Contribution of the HisRS C-Terminal Domain to the Pyrophosphate Exchange and Aminoacylation Reaction[a]

| substrate | operational rate constant | relative $k_A/k_B$ | $-\Delta G^{\ddagger}$ (kcal $mol^{-1}$) |
|---|---|---|---|
| $tRNA^{His}_{GUG}$ | $k$(HisRS AA)/$k$($N_{cat}$ HisRS AA) | $1.6 \times 10^2$ | 3.1 |
| U73 $tRNA^{His}_{GUG}$ | $k$(HisRS AA)/$k$($N_{cat}$ HisRS AA) | 5.8 | 1.1 |
| $tRNA^{His}_{CUA}$ | $k$(HisRS AA)/$k$($N_{cat}$ HisRS AA) | $2.3 \times 10^2$ | 3.3 |
| $microhelix^{His}$ | $k$(HisRS AA)/$k$($N_{cat}$ HisRS AA) | $2.6 \times 10^2$ | 3.4 |
| histidine | $k$(HisRS−$PP_i$ exchange)/$k$($N_{cat}$ HisRS−$PP_i$ exchange) | $2.4 \times 10^3$ | 4.8 |
| ATP | $k$(HisRS−$PP_i$ exchange)/$k$($N_{cat}$ HisRS−$PP_i$ exchange) | $7.8 \times 10^2$ | 4.1 |

[a] The values of relative $k_A/k_B$ were determined from values of $k_{cat}/K_m$ for the indicated enzyme and substrate, where AA refers to the aminoacylation reaction and $PP_i$ refers to the $PP_i$ exchange reaction using parameters from Tables 1 and 2 and Yan et al. (1996). The difference in apparent free energy of activation $-\Delta\Delta G^{\ddagger}$ was calculated according to the equation $\Delta\Delta G = -RT \ln(k_A/k_B)$, where $T$= 310 K and $R$ = 1.987 cal K $mol^{-1}$ (Fersht, 1985).

## DISCUSSION

In the years before comprehensive structural information was available, evidence for the modular nature of the aaRS was provided by efforts to generate stable subfragments through the use of limited proteolysis and gene deletion (Kohda et al., 1987; Jasin et al., 1983). Functional subdomains on the order of 300 (MetRS) and 460 residues (AlaRS) were obtained using these respective techniques, and the resulting truncated enzymes were found to possess full pyrophosphate exchange activity but diminished aminoacylation activity. Crystal structures of aaRS were subsequently exploited to guide further domain truncation and cleavage experiments, including efforts to bisect MetRS (Burbaum & Schimmel, 1991), attempts to define a minimalist GlnRS by *in vivo* complementation (Schwob & Söll, 1993), and the construction of truncated versions of SerRS in which the N-terminal coiled-coil domain had been shortened or deleted (Borel et al., 1994).

The results described here for the histidine system differ from those of the previous studies in several key respects. By use of the crystal structure of HisRS from *E. coli*, rational break points within the flexible linker that separates the two domains were identified, allowing the use of molecular biology to express each domain independently. Although expression of both catalytic (Kohda et al., 1987; Jasin et al., 1983; Borel et al., 1994) and individual tRNA binding domains (Gale & Schimmel, 1995; Commans et al., 1995) has been successful, HisRS is the first aaRS for which expression and purification of both major domains have been accomplished. The relatively high stability of $N_{cat}$ HisRS *in vivo* (Figure 2) and $C_{ter}$ HisRS *in vitro* suggests that each retains the global fold observed within the context of the full-length native enzyme. Further evidence for the stability of $N_{cat}$ HisRS is provided by the observation that $K_m^{ATP}$, $K_m^{His}$, and $K_m^{tRNA}$ were all within a factor of 2 of that of the full-length enzyme (Tables 1 and 2).

In contrast to the AlaRS, MetRS, and SerRS truncated proteins, $N_{cat}$ HisRS exhibited a greater decrease in adenylation than in aminoacylation. This 1.5 kcal mol$^{-1}$ difference in apparent transition state free energy between the two reactions (Table 3) may be significant, given that HisRS is converted into a monomer upon removal of the C-terminal domain. Although both prokaryotic AlaRS and MetRS are converted to monomeric enzymes upon deletion of C-terminal sequences, in neither system does subunit association play a major role in catalytic function (Buechter & Schimmel, 1993; Cassio & Waller, 1971). Interestingly, while the human AlaRS maintains 41% identity with the N-terminal catalytic core of the *E. coli* enzyme, it lacks the C-terminal sequences essential for tetramer formation found in the prokaryotic AlaRS (Shiba et al., 1995). By contrast, the reduced catalytic activity of $N_{cat}$ HisRS suggests that subunit interactions are important for both the adenylation and aminoacylation reactions, perhaps by virtue of their effect on motif 2. Such an effect could arise out of the requirement for the intersubunit contact between Gln 124 and Pro 44 in achieving proper stabilization of the motif 2 loop (Eriani et al., 1993; Arnez et al., 1995).

A second functionally important difference between $N_{cat}$ HisRS and the other truncated aaRS is the apparent retention of specificity for cognate tRNA. Both SerRS and GlnRS show an increased propensity to mischarge noncognate tRNAs when one or more accessory domains are deleted (Borel et al., 1994; Schwob & Söll, 1993), but AlaRS retains G3·U70-dependent aminoacylation when truncated to a 461-residue polypeptide (Buechter & Schimmel, 1995). These functional differences in the retention of specificity may be explained in part by the relative contribution of acceptor stem recognition to that of the full-length tRNA. For both HisRS and AlaRS, the loss in free energy of activation upon truncating the full-length tRNA to a microhelix is on the order of 3−4 kcal mol$^{-1}$ (Francklyn et al., 1992, this work), while for the seryl and glutaminyl systems, the loss is on the order of 8 and 10 kcal mol$^{-1}$, respectively (Sampson & Saks, 1993; Wright et al., 1993). The significance of acceptor stem recognition in the former systems is a direct consequence of the crucial G1·C73 and G3·U70 determinants, which are required for histidine specific and alanine specific aminoacylation, respectively (Hou & Schimmel, 1988; McClain & Foss, 1988; Himeno et al., 1989; Francklyn & Schimmel, 1990). For the seryl system, the extra arm serves as a major determinant, and the loss of transition state stabilization associated with its deletion (5.9 kcal mol$^{-1}$) is very nearly equal to the free energy lost (6.5 kcal mol$^{-1}$) upon deletion of the coiled-coil domain that forms the major accessory domain of SerRS (Sampson & Saks, 1993; Borel et al., 1994).

Despite the absence of mischarging of noncognate tRNAs, $N_{cat}$ HisRS did show significantly reduced discrimination between C and U at the discriminator nucleotide (N73). Thus, one important function of the C-terminal domain may be to provide additional recognition specificity for G1·C73, perhaps through a mechanism in which recognition of the two main tRNA domains is coupled. The negative cooperativity of the recognition of the acceptor stem and the anticodon was previously noted in the analysis of HisRS mutants selected on the basis of preferential interactions with a U73 $tRNA^{His}$ suppressor *in vivo* (Yan et al., 1996). The C-terminal domain−N-terminal domain interface may therefore serve to structurally integrate the recognition of the acceptor stem and the anticodon, ultimately enhancing or stabilizing necessary conformational changes associated with motif 2 and the catalytic residues therein (Cusack et al., 1996).

The somewhat surprising retention of specificity for anticodon sequences by $N_{cat}$ HisRS raises the possibility that, even in the context of the truncated protein, interactions with the cognate tRNA outside of the acceptor stem can provide a small (1.5 kcal mol$^{-1}$) but significant contribution toward decreasing the free energy of the transition state. [For truncated versions of AlaRS, the full-length tRNA and minihelix are aminoacylated with nearly the same efficiency, suggesting that interactions outside the acceptor stem are less important than those in the histidine system (Beuchter, 1995).] One possibility is that the catalytic domain itself is responsible for direct interaction with the anticodon nucleotide. None of the data presented here rule out this model, but it would require major revision of the accepted models for the class II aaRS−tRNA interaction (Arnez & Moras, 1995; Cusack, 1993). Based on our previous suggestion that direct interactions with the anticodon are made by the C-terminal domain (Arnez et al., 1995), this ability to discriminate between tRNAs differing at their anticodon sequences would have to be rationalized on the basis of an indirect effect, in which an altered structure imparted by the CUA anticodon created one or more unfavorable interactions

with the dimerized N-terminal domain. A similar distance effect has been proposed to account for the ability of mutations in the D stem to affect the anticodon−codon interaction during translation (Yarus, 1979).

A recurring observation is that rejection of noncognate tRNAs and the reduced aminoacylation of cognate tRNAs with recognition nucleotide substitutions is reflected in the preferential reduction of $k_{cat}$ versus increases in $K_m$ (Ebel et al., 1973). A preferential decrease in $k_{cat}$ is also observed upon the loss of the C-terminal domain of HisRS, and such decreases are the signature of a classical principle of enzymology, namely the utilization of substrate binding energy to lower the free energy of the transition state (Jencks, 1975; Fersht, 1985). The free energy comparisons presented here and by others (Francklyn et al., 1992; Sampson & Saks, 1993; Buechter & Schimmel, 1993; Frugier et al., 1994) raise the possibility that the utilization of binding energy to lower the transition state may be a general mechanism by which the aaRSs both efficiently catalyze the aminoacylation reaction and discriminate against noncognate substrates. For example, if all of the 2700 Å$^2$ calculated buried surface of the GlnRS−tRNA$^{Gln}$ interaction (Rould et al., 1991) contributed strictly to binding interactions, the dissociation of the tRNA would be far too slow to support the required physiological rate of protein synthesis. Evolution of the aaRS may therefore have involved increases in $K_m$ for tRNA from an initially very small value to the parameter values on the order of 0.1−1.0 $\mu$M which are characteristic of the modern enzymes (Fersht, 1985). A necessary part of this evolution would entail the optimization of interactions with the transition state at the expense of tight binding to the tRNA in its initially bound state. The accessory domains appended to the catalytic core may therefore contribute structural elements that allow binding energy realized from a productive interaction with the cognate tRNA to be coupled to the lowering of $\Delta G^{\ddagger}$. Such a mechanism would provide a substantial rate enhancement and would account for the relatively high $K_m^{tRNA}$ parameters which are characteristic of the aaRS. Given the idiosyncratic distribution of tRNA recognition elements in different systems, the observed diversity of accessory domains may reflect an array of different structural solutions that act through a common energetic mechanism. Ultimately, the values of $K_m$ observed also reflect selective pressure toward the *in vivo* concentrations of the appropriate isoacceptors, allowing the activity of these enzymes to be regulated over a biologically significant concentration range.

The three classical pathways by which binding energy is used to lower the transition state are strain, induced fit, and nonproductive binding (Jencks, 1975). In the complexes of both GlnRS and AspRS with their cognate tRNAs, the anticodon loops undergo considerable deformation upon binding (Rould et al., 1991; Cavarelli et al., 1993), behavior analogous to the classical definition of strain. The melting of the U1·A72 base pair of tRNA$^{Gln}$ upon binding (Rould et al., 1991) constitutes a second example of strain, and the ability of tRNAs to undergo this deformation has been shown to influence tRNA selection by GlnRS (Rogers & Söll, 1990). Evidence is also accumulating for the importance of induced fit on the part of the enzymes, particularly for class I GlnRS (Ibba et al., 1996) and class II SerRS (Cusack et al., 1996). For the latter, the crucial motif 2 loop undergoes a conformational change upon tRNA binding in which a conserved motif 2 glutamate switches from a contact with the N7 of ATP to a contact with the N73 of the tRNA. These examples illustrate the general principle of using binding energy to drive conformational changes on the part of either tRNA or aaRS, and it is likely that further work will show how such changes are required for properly orienting catalytic groups. Because productive interactions are likely to promote such changes most efficiently, this provides an explicit connection between tRNA specificity and catalysis.

The data presented here demonstrate that a primitive enzyme of 300−350 amino acids based on the class II catalytic fold that possessed all three class-defining signature motifs could have possessed significant catalytic activity for both the adenylation and aminoacylation reactions. By virtue of retaining a high degree of selectivity for acceptor stem nucleotides, such a primitive enzyme could also have possessed considerable specificity for a limited set of corresponding RNA adapter molecules, which may or may not have resembled modern day tRNAs. These properties are consistent with the expectations of the "operational RNA code model" (Schimmel et al., 1993), but the discrimination by $N_{cat}$ HisRS between the full-length and microhelix RNA implies that, for at least some systems, RNAs possessing a tertiary fold are better aminoacylation substrates for the core catalytic domains than RNAs based on a simple duplex. Along these lines, it is intriguing that HisRS retains the ability to aminoacylate an impressive array of non-tRNA structures, including viral RNAs, pseudoknot structures derived from them (Felden et al., 1994; Rudinger et al., 1992), and 10S RNA (K. Keiler, personal communication). Moreover, the HisRS fold forms an essential subdomain of the translational regulatory protein GCN-2, which possesses a considerably broader tRNA binding specificity than the yeast HisRS to which it is most closely related (Wek et al., 1989). Further studies of the structural relationships between the accessory domains of aaRS and their significance for tRNA recognition may be informative with regard to the origin of the genetic code and its connection to aaRS evolution. On the basis of the information obtained thus far from HisRS and other aaRSs, additional surprises are likely to be in store.

## ACKNOWLEDGMENT

We thank the NHLB1 Automated Molecular Biology Multi-User Facility for conducting the automated DNA sequencing analysis, B. Lyons for assistance in the collection and analysis of NMR data, and P. Schimmel and K. Musier-Forsyth for their helpful suggestions on the manuscript.

## REFERENCES

Arnez, J. G., & Moras, D. (1995) in *RNA-Protein Interactions* (Mattaj, I. A., & Nagai, K., Eds.) pp 52−81, IRL Press, Oxford.
Arnez, J. G., Harris, D. C., Mitschler, A., Rees, B., Francklyn, C. S., & Moras, D. (1995) *EMBO J. 14*, 4143−4155.
Biou, V., Yaremchuk, A., Tukalo, M., & Cusack, S. (1994) *Science 263*, 1401−1410.
Borel, F., Vincent, C., Leberman, R., & Hartlein, M. (1994) *Nucleic Acids Res. 15*, 2963−2969.
Buechter, D., & Schimmel, P. (1993) *Biochemistry 32*, 5267−5272.
Buechter, D., & Schimmel, P. (1995) *Biochemistry 34*, 6014−6019.
Burbaum, J., & Schimmel, P. (1991) *Biochemistry 30*, 319−324.
Calender, R., & Berg, P. (1966) *Biochemistry 5*, 1690−1695.
Carter, C. W. (1993) *Annu. Rev. Biochem. 62*, 715−748.
Cassio, D., & Waller, J.-P. (1971) *Eur. J. Biochem. 20*, 283−300.

Cavarelli, J., Rees, B., Ruff, M., Thierry, J. C., & Moras, D. (1993) *Nature 362*, 181−184.
Commans, S., Plateau, P., Blanquet, S., & Dardel, F. (1995) *J. Mol. Biol. 253*, 100−113.
Cusack, S. (1993) *Biochimie 75*, 1077−1081.
Cusack, S. (1995) *Nat. Struct. Biol. 2*, 824−831.
Cusack, S., Berthet-Colominas, C., Hartlein, M., Nassar, N., & Leberman, R. (1990) *Nature 347*, 249−255.
Cusack, S., Härtlein, M., & Leberman, R. (1991) *Nucleic Acids Res. 19*, 3489−3498.
Cusack, S., Yaremchuk, A., & Tukalo, M. (1996) *EMBO J. 15*, 2834−2842.
Delarue, M. (1995) *Curr. Opin. Struct. Biol. 5*, 48−55.
Delarue, M., & Moras, D. (1993) *BioEssays 15*, 1−13.
Ebel, J. P., Giege, R., Bonnet, J., Kern, D., Befort, N., Bollack, C., Fasiolo, F., Gangloff, J., & Dirheimer, G. (1973) *Biochimie 55*, 547−577.
Eriani, G., Cavarelli, J., Martin, F., Dirheimer, G., Moras, D., & Gangloff, J. (1993) *Proc. Natl. Acad. Sci. U.S.A. 90*, 10816−10820.
Felden, B., Florentz, C., McPherson, A., & Giege, R. (1994) *Nucleic Acids Res. 22*, 2882−2886.
Fersht, A. R. (1977) *Biochemistry 16*, 1025−1030.
Fersht, A. R. (1985) *Enzyme Structure and Mechanism*, 2nd ed., W. H. Freeman and Company, San Francisco.
Fersht, A. R., Ashford, J. S., Bruton, C. J., Jakes, R., Koch, G. L. E., & Hartley, B. S. (1975) *Biochemistry 14*, 1−4.
Francklyn, C., & Schimmel, P. (1990) *Proc. Natl. Acad. Sci. U.S.A. 87*, 8655−8659.
Francklyn, C., Shi, J.-P., & Schimmel, P. (1992) *Science 255*, 1121−1125.
Frugier, M., Florentz, C., & Giegé, R. (1994) *EMBO J. 13*, 2218−2226.
Gale, A., & Schimmel, P. (1995) *Biochemistry 34*, 8896−8903.
Gill, S. C., & von Hippel, P. H. (1989) *Anal. Biochem. 182*, 319−326.
Grodberg, J., & Dunn, J. (1988) *J. Bacteriol. 170*, 1245−1253.
Himeno, H., Hasegawa, T., Ueda, T., Watanabe, K., Miura, K., & Shimizu, M. (1989) *Nucleic Acids Res. 17*, 7855−7862.
Hou, Y. M., & Schimmel, P. (1988) *Nature 333*, 140−145.
Ibba, M., Hong, K.-W., Sherman, I., Sever, S., & Söll, D. (1996) *Proc. Natl. Acad. Sci. U.S.A. 93*, 6953−6958.
Jasin, M., Regan, L., & Schimmel, P. (1983) *Nature 306*, 441−447.
Jeener, J., Meier, B. H., Bachmann, P., & Ernst, R. R. (1979) *J. Chem. Phys. 71*, 4546−4553.
Jencks, W. P. (1975) *Adv. Enzymol. 43*, 219−410.
Kohda, D., Yokoyama, S., & Miyazawa, T. (1987) *J. Biol. Chem. 262*, 558−563.
Landes, C., Perona, J., Brunie, S., Rould, M., Zelwer, C., Steitz, T., & Risler, J. (1995) *Biochimie 77*, 194−203.
Logan, D. T., Mazauric, M.-H., Kern, D., & Moras, D. (1995) *EMBO J. 14*, 4156−4167.
Martinis, S. A., & Schimmel, P. (1995) in *tRNA: Structure, Biosynthesis, and Function* (Söll, D., & Rajbhandary, U., Eds.) pp 349−370, American Society for Microbiology, Washington, DC.
McClain, W. H., & Foss, K. (1988) *Science 240*, 793−796.
Nagel, G. M., & Doolittle, R. F. (1991) *Proc. Natl. Acad. Sci. U.S.A. 88*, 8121−8125.
Onesti, S., Miller, A. D., & Brick, P. (1995) *Structure 3*, 163−176.
Rogers, M. J., & Söll, D. (1990) *Prog. Nucleic Acid Res. Mol. Biol. 39*, 185−208.
Rould, M. A., Perona, J. J., Söll, D., & Steitz, T. A. (1989) *Science 246*, 1135−1142.
Rould, M. A., Perona, J. J., & Steitz, T. A. (1991) *Nature 352*, 213−218.
Rudinger, J., Florentz, C., Dreher, T., & Giege, R. (1992) *Nucleic Acids Res. 20*, 1865−1870.
Saks, M. E., & Sampson, J. R. (1996) *EMBO J. 15*, 2843−2849.
Sampson, J. R., & Saks, M. E. (1993) *Nucleic Acids Res. 19*, 4467−4475.
Schimmel, P., & Söll, D. (1979) *Annu. Rev. Biochem. 48*, 601−648.
Schimmel, P., Giege, R., Moras, D., & Yokoyama, S. (1993) *Proc. Natl. Acad. Sci. U.S.A. 90*, 8763−8768.
Schmidt, E., & Schimmel, P. (1995) *Biochemistry 34*, 11204−11210.
Schwob, E., & Söll, D. (1993) *EMBO J. 12*, 5201−5208.
Shiba, K., Ripmaster, T., Suzuki, N., Nichols, R., Plotz, P., Noda, T., & Schimmel, P. (1995) *Biochemistry 34*, 10340−10349.
Wek, R. C., Jackson, B. M., & Hinnebusch, A. G. (1989) *Proc. Natl. Acad. Sci. U.S.A. 86*, 4579−4583.
Wright, D. J., Martinis, S. A., Jahn, M., Söll, D., & Schimmel, P. (1993) *Biochimie 75*, 1041−1049.
Yan, W., & Francklyn, C. (1994) *J. Biol. Chem. 269*, 10022−10027.
Yan, W., Augustine, J., & Francklyn, C. (1996) *Biochemistry 35*, 6559−6568.
Yarus, M. (1979) *Prog. Nucleic Acid Res. Mol. Biol. 23*, 195−225.

BI962395Y